


Quantized Nonlinear Conductance in Ballistic Metals

C. L. Kane *Department of Physics and Astronomy, University of Pennsylvania, Philadelphia, Pennsylvania 19104, USA* (Received 12 August 2021; revised 11 January 2022; accepted 12 January 2022; published 16 February 2022)

We introduce a nonlinear frequency-dependent $D + 1$ terminal conductance that characterizes a D -dimensional Fermi gas, generalizing the Landauer conductance in $D = 1$. For a 2D ballistic conductor, we show that this conductance is quantized and probes the Euler characteristic of the Fermi sea. We critically address the roles of electrical contacts and Fermi liquid interactions, and we propose experiments on 2D Dirac materials, such as graphene, using a triple point contact geometry.

DOI: [10.1103/PhysRevLett.128.076801](https://doi.org/10.1103/PhysRevLett.128.076801)

A dramatic consequence of the role of topology in the structure of quantum matter is the existence of topological invariants that are reflected in quantized response functions. The hallmark of this is the integer quantized Hall effect (IQHE) [1], which probes the Chern number characterizing the topology of a gapped two-dimensional (2D) electronic phase [2]. Quantum topology also plays a role in the electrical response of metals. For example, the Berry phase associated with the Fermi surface of a 2D metal contributes to an intrinsic nonquantized part of the anomalous Hall conductivity [3]. In 3D, the Chern number associated with the Fermi surface in a Weyl semimetal leads to a quantized circular photogalvanic effect [4] in the absence of disorder and interactions [5]. In addition to the quantum topology associated with the twisting of the quantum states on the Fermi surface, metals also exhibit a simpler geometric topology associated with the Fermi surface. It is well known that noble metals, like copper, have a Fermi surface with a nontrivial genus [6]. While Fermi surfaces have been mapped in detail, and Lifshitz transitions [7] where their topology changes have been characterized [8,9], Fermi surface topology has not been measured directly. Here we pose the question of whether the topology of the Fermi surface is associated with a quantized response.

An indication that the answer is affirmative is provided by the 1D case. The Landauer conductance of a ballistic 1D conductor is e^2/h times the number of occupied bands [10,11]. While this quantization is related to the IQHE, there are important differences. First, it is less robust, since it relies on reflectionless contacts and the absence of scattering. Nonetheless, conductance quantization has been observed in quantum point contacts [12], 1D semiconductor wires [13,14], and carbon nanotubes [15], albeit with less precision than the IQHE. A second difference is that, unlike the IQHE, the quantized value does not reflect the topology of a 2D gapped state, but rather the topology of the 1D filled Fermi sea.

In this Letter, we seek to generalize this to higher dimensions. For a D -dimensional ballistic conductor with suitably defined ideal leads, we introduce a $D + 1$ terminal frequency-dependent nonlinear conductance,

$$I_{D+1}(\omega_\Sigma) = G(\{\omega_p\}) \prod_{p=1}^D V_p(\omega_p), \quad (1)$$

where $I_p(\omega_p)$ [$V_p(\omega_p)$] are the current (voltage) in lead p at frequency ω_p and $\omega_\Sigma = \sum_p \omega_p$. We will show that for $D = 1$ and 2, $G(\{\omega_p\})$ has a universal term of the form

$$G(\{\omega_p\}) = \frac{i\omega_\Sigma}{\prod_p (i\omega_p)} \frac{e^{D+1}}{h^D} \chi_F, \quad (2)$$

where χ_F is the *Euler characteristic* of the D -dimensional Fermi sea. We will focus on $D = 2$, leaving the generalization to $D > 2$ to future work. This result will be established for noninteracting electrons by first presenting a simple thought experiment, which is formalized by a semiclassical Boltzmann transport theory. This will be followed by a more general quantum nonlinear response theory, which reproduces the Boltzmann theory. We will then critically assess the prospects for experimentally measuring χ_F in a 2D conductor using a triple point contact. Crucial issues to be addressed include the role of electrical contacts and electron-electron interactions, which place bounds on the applicability of (2).

The Euler characteristic is defined as [16]

$$\chi_F = \sum_{l=0}^D (-1)^l b_l, \quad (3)$$

where b_l is the l th Betti number, given by the rank of the l th homology group, which counts the topologically distinct l cycles. In 1D, χ_F is the number of disconnected components of the Fermi sea. In general, χ_F can be expressed as a

sum over the disconnected components of the Fermi surface. In 2D, electron-like, hole-like, and open Fermi surfaces contribute $+1$, -1 , and 0 , respectively. In 3D, each Fermi surface with genus g_k contributes $1 - g_k$. Note that completely empty bands and completely filled bands both have $\chi_F = 0$, and electron- and hole-like Fermi surfaces have opposite sign for even D .

Morse theory [17,18] provides a representation of χ_F in terms of the critical points of the electronic dispersion $E(\mathbf{k})$, where $\mathbf{v}_k = \nabla_{\mathbf{k}} E(\mathbf{k})/\hbar = 0$ for $E(\mathbf{k}) < E_F$,

$$\chi_F = \sum_m \eta_m, \quad (4)$$

where m labels the critical points (assumed nondegenerate) with signature $\eta_m = \text{sgn}\{\det[\partial^2 E(\mathbf{k}_m)/\partial k_i \partial k_j]\}$. This shows that χ_F changes at a Lifshitz transition [7], when a minimum, maximum, or saddle point passes through E_F , signaling a change in Fermi surface topology.

To motivate our result, we review and then generalize a thought experiment [19] that explains the quantization of the 1D Landauer conductance. Consider an infinitely long 1D electron gas (1DEG), with electronic states $E(k) = \hbar^2 k^2/2m$ filled to E_F . Apply an h/e voltage pulse $V(t)$ by introducing a slowly varying electric field $E(x, t)$ that is nonzero near $x = 0$ and $t = 0$, such that $\int dx dt E(x, t) = h/e$. This will lead to a charge $Q = Gh/e$ transferred into the right lead, where G is the conductance. The charge $Q = e$ can be deduced from the fact that the impulse $V(t)$ transfers precisely one electron between the left- and right-moving Fermi points, reflecting the chiral anomaly associated with 1D chiral fermions. The chiral anomaly is a consequence of the fact that the right and left movers are connected at the critical point $k = 0$. Because of the impulse, one electron crosses $k = 0$ and changes direction. This argument can be generalized to a more complicated dispersion $E(k)$. An electron will change direction at every critical point inside the Fermi sea, leading to a net transferred charge $Q = e\chi_F$, with χ_F given in (4). It follows that $G = \chi_F e^2/h$.

We now seek a version of this argument for $D = 2$. Consider a 2D electron gas (2DEG) with dispersion $E(\mathbf{k})$ defined on an infinite plane that is divided into three regions that meet at a point. Apply an h/e pulse $V_1(t)$ to region 1, followed by an h/e pulse $V_2(t)$ to region 2 by introducing electric fields near their boundaries. Each pulse will lead to a charge transferred to lead 3 that scales with the length of the contact. However, we will argue that the excess charge Q_3 , defined as the charge transferred due to the two pulses with the charge transferred for independent pulses subtracted off, will be universal and given by $Q_3 = e\chi_F$, where χ_F is the Euler characteristic of the 2D Fermi sea. This excess charge defines a second-order nonlinear response that can be isolated in the frequency domain.

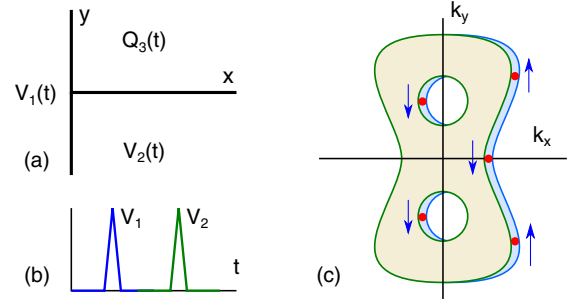


FIG. 1. (a),(b) A thought experiment in which h/e voltage pulses are applied to regions 1 and 2 in (a). (c) A hypothetical 2D Fermi sea with $\chi_F = -1$. After pulse $V_1(t)$ for $x > 0$, there are extra electrons (shown in blue) propagating to the right. Pulse $V_2(t)$ accelerates those electrons, and v_y changes sign at the points indicated by the red dots in a direction indicated by the arrows. The net excess charge in region 3 is determined by the difference between the number of concave and convex critical points on the Fermi surface with $\mathbf{v}_k \propto +\hat{x}$, which measures χ_F .

It is simplest to consider the geometry in Fig. 1(a), where region 1 is the half-plane $x < 0$, and regions 2 (3) are the quadrants $x > 0, y < 0$ ($y > 0$). In that case, the $V_1(t)$ pulse accelerates electrons in the x direction, so that for every value of k_y on the Fermi surface there is one extra electron propagating to the right ($v_x > 0$) for $x > 0$ and one extra hole propagating to the left ($v_x < 0$) for $x < 0$. Q_3 will be determined by the effect of the $V_2(t)$ pulse on those extra electrons with $x > 0$, which are accelerated in the y direction. As in the 1D example discussed above, the transferred charge can be determined by counting those electrons that change directions at the critical points on the Fermi surface where $v_x > 0$ and $v_y = 0$. Referring to the hypothetical Fermi surface in Fig. 1(c), these arise at the points indicated by the dots, which come in two varieties distinguished by whether the Fermi surface is concave (convex) with $\partial^2 E/\partial k_y^2 > 0$ (< 0). Q_3 is then e times the sum over those critical points with signs $\text{sgn}[\partial^2 E/\partial k_y^2]$. By inspecting Fig. 1(c), it is clear that this is χ_F . This will be proven below. We conclude that $Q_3 = e\chi_F$.

The above argument can be sharpened by developing a semiclassical Boltzmann transport theory. In the absence of scattering, the electron distribution function $f(\mathbf{k}, \mathbf{r}, t)$ satisfies the collisionless Boltzmann equation

$$(\partial/\partial t + \mathbf{v}_k \cdot \nabla_{\mathbf{r}} + e\mathbf{E} \cdot \nabla_{\mathbf{k}}/\hbar)f = 0. \quad (5)$$

Consider two weak pulses, $\mathbf{E}_1(x_1, y_1, t) = \xi_1 \delta(t - t_1) \delta(x_1) \hat{x}$ and $\mathbf{E}_2(x_2, y_2, t) = \xi_2 \delta(t - t_2) [\delta(y_2) \theta(x_2) \hat{y} - \delta(x_2) \theta(-y_2) \hat{x}]$. We compute the charge

$$Q_3(t_3) = e \int \frac{d^2 k}{(2\pi)^2} \int_0^\infty dx_3 dy_3 \delta f(\mathbf{k}, x_3, y_3, t_3) \quad (6)$$

perturbatively at order $\xi_1\xi_2$ for $t_1 < t_2 < t_3$. Integrating (5) to this order gives $\delta f = e^2\xi_1\xi_2\delta\tilde{f}/\hbar^2$ with

$$\delta\tilde{f} = \int dy_1 dx_2 \delta(\mathbf{r}_{32} - \mathbf{v}_k t_{32}) \frac{\partial}{\partial k_y} \left[\delta(\mathbf{r}_{21} - \mathbf{v}_k t_{21}) \frac{\partial f_0}{\partial k_x} \right], \quad (7)$$

where $f_0(\mathbf{k}) = \theta[E_F - E(\mathbf{k})]$, $t_{ij} = t_i - t_j$, $\mathbf{r}_{32} = (x_3 - x_2, y_3)$, $\mathbf{r}_{21} = (x_2, -y_1)$, and $x_2(y_1)$ are integrated from 0 ($-\infty$) to ∞ . The second term in \mathbf{E}_2 , with $x_2 = 0$, is absent because the δ functions cannot be satisfied. After plugging (7) into (6), the four spatial integrals cancel the δ functions, but since $x_2 > 0$ ($y_3 > 0$), we require $v_x > 0$ ($v_y > 0$) inside (outside) $\partial/\partial k_y$. After integrating by parts on k_y and replacing $\xi_{1,2} \rightarrow h/e$, we obtain

$$Q_3 = -e \int d^2k \frac{\partial f_0(\mathbf{k})}{\partial k_x} \theta[v_x(\mathbf{k})] \frac{\partial \theta[v_y(\mathbf{k})]}{\partial k_y}. \quad (8)$$

This captures the result of the heuristic argument above: $-\partial f_0/\partial k_x$ isolates the Fermi surface, while $\theta(v_x)\partial[\theta(v_y)]/\partial k_y$ isolates the critical points on the Fermi surface identified in Fig. 1(c). To make contact with Eq. (4), it is convenient to add zero to the integrand in the form $-(\partial f_0/\partial k_y)\theta(v_x)\partial\theta(v_y)/\partial k_x$. This is clearly zero, since $\partial f_0/\partial k_y = v_y \partial f_0/\partial E$, and $\partial\theta(v_y)/\partial k_x$ fixes $v_y = 0$. This allows us to integrate by parts to obtain

$$Q_3 = e \int d^2k f_0(\mathbf{k}) \left[\frac{\partial\theta(v_x)}{\partial k_x} \frac{\partial\theta(v_y)}{\partial k_y} - \frac{\partial\theta(v_x)}{\partial k_y} \frac{\partial\theta(v_y)}{\partial k_x} \right]. \quad (9)$$

The integrand is only nonzero near critical points where $v_x = v_y = 0$. The integral evaluates the signature of each critical point, leading to

$$Q_3 = e \sum_m \eta_m = e\chi_F. \quad (10)$$

We next consider the frequency domain response. This can be computed using the Boltzmann theory; however, we will first formulate a more general quantum nonlinear response theory and show the Boltzmann theory follows, provided the applied fields vary slowly in space and time. To this end, we introduce the Hamiltonian

$$\mathcal{H} = \mathcal{H}_0 + (V_1 \hat{Q}_1 e^{(\eta-i\omega_1)t} + V_2 \hat{Q}_2 e^{(\eta-i\omega_2)t} + \text{H.c.}), \quad (11)$$

with $\mathcal{H}_0 = \sum_{\mathbf{k}} E(\mathbf{k}) c_{\mathbf{k}}^\dagger c_{\mathbf{k}}$ and $\hat{Q}_p = \int d\mathbf{r} Q_p(\mathbf{r}) \rho(\mathbf{r})$ is defined in terms of the density operator $\rho(\mathbf{r})$ for each of the three regions in Fig. 1(a). $Q_p(\mathbf{r})$ is 1 (0) inside (outside) region p and is assumed to transition smoothly between 1 and 0 in a width b near the boundary, with $k_F b \gg 1$.

We compute the charge $Q_3(t)$ at frequency $\omega_1 + \omega_2$ to order $V_1 V_2$. We adopt a scalar potential formulation, which

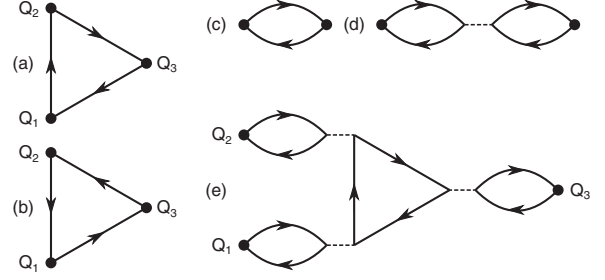


FIG. 2. Feynman diagrams for the conductance. (a),(b) The 2D nonlinear conductance and (c) the 1D linear conductance in the absence of interactions and the quantized conductance determined by χ_F . (d),(e) Corrections to (a)–(c) that describe screening due to electron interactions and modify the quantized result.

avoids the diamagnetic term. The response has a structure similar to second-order nonlinear optical response [20–22] and is determined by evaluating the Feynman diagrams in Figs. 2(a) and 2(b),

$$Q_3(\omega_1 + \omega_2) = \alpha(\omega_1, \omega_2) V_1 V_2, \quad (12)$$

with

$$\alpha(\omega_1, \omega_2) = \frac{e^3}{\hbar^2} \sum_{l,m,n} \frac{f_l - f_m}{\omega_1 - \omega_{lm} + i\eta} \left[\frac{Q_1^{lm} Q_2^{mn} Q_3^{nl}}{\omega_1 + \omega_2 - \omega_{ln} + i\eta} - \frac{Q_1^{lm} Q_3^{mn} Q_2^{nl}}{\omega_1 + \omega_2 - \omega_{nm} + i\eta} \right] + (1 \leftrightarrow 2). \quad (13)$$

Here l, m , and n label momenta, $\omega_{lm} = [E(\mathbf{k}_l) - E(\mathbf{k}_m)]/\hbar$, $f_l = f_0(\mathbf{k}_l)$ is a Fermi function, and

$$Q_p^{lm} = \langle \mathbf{k}_l | \hat{Q}_p | \mathbf{k}_m \rangle = \int d\mathbf{r}_p Q_p(\mathbf{r}_p) e^{i\mathbf{q}_{lm} \cdot \mathbf{r}_p} \quad (14)$$

with $\mathbf{q}_{lm} = \mathbf{k}_l - \mathbf{k}_m$. Since $Q_p(\mathbf{r})$ varies on the scale of b , an expansion in \mathbf{q}_{lm} and \mathbf{q}_{nm} is justified. As shown in Supplemental Material Sec. A [23], the \mathbf{q}_{lm} and \mathbf{q}_{nm} integrals can be performed to obtain

$$\alpha = \int \frac{d^2\mathbf{k} d^6\mathbf{r}_{1,2,3}}{(2\pi)^2} \nabla_{\mathbf{r}}^a Q_1(\mathbf{r}_1) \nabla_{\mathbf{r}}^b Q_2(\mathbf{r}_2) Q_3(\mathbf{r}_3) [\nabla_{\mathbf{k}}^a f_0(\mathbf{k}) D(\mathbf{r}_{21}, \mathbf{k}, \omega_1) \nabla_{\mathbf{k}}^b D(\mathbf{r}_{32}, \mathbf{k}, \omega_1 + \omega_2)] + (1 \leftrightarrow 2), \quad (15)$$

with $D(\mathbf{r}, \mathbf{k}, \omega) = e^{-(\eta-i\omega)|\mathbf{r}|/|\mathbf{v}_k|} \delta(\mathbf{r} \times \mathbf{v}_k) \theta(\mathbf{r} \cdot \mathbf{v}_k)$. This form of the response also follows from solving (5) in the frequency domain with $\mathbf{E}_p(\mathbf{r}, t) = -\nabla Q_p(\mathbf{r}) V_p e^{(\eta-i\omega_p)t}$.

In Supplemental Material Sec. B [23], we evaluate (15) for the infinite plane in which three rays separate regions that subtend angles φ_p (see Fig. 3). We show that there is an intrinsic term $\alpha_i(\omega_1, \omega_2) = \chi_F(e^3/h^2)/(\eta - i\omega_1)(\eta - i\omega_2)$ that is independent of φ_p (provided all $\varphi_p < \pi$ [24]), as well as the detailed spatial profile of the fields. In addition, there

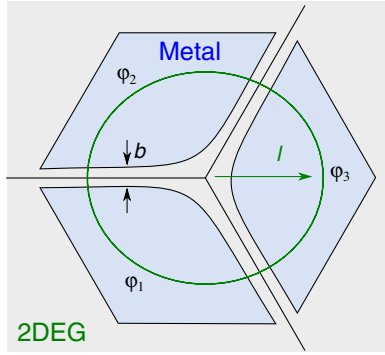


FIG. 3. A triple point contact as a model experimental geometry. A 2D electron gas is connected to three metallic leads of size larger than the tunneling mean free path ℓ . The leads are separated by b and subtend angles $\varphi_{1,2,3}$.

is an extrinsic term with a distinct frequency dependence, $\alpha_e(\omega_1, \omega_2) = k(e^3/h^2)/[\eta - i(\omega_1 + \omega_2)]^2$ with a coefficient k that depends on φ_p as well as the details of the Fermi surface. The extrinsic term was not picked up by the pulse argument (where we assumed $t_2 > t_1$), since it arises when \mathbf{E}_1 and \mathbf{E}_2 coincide in time. The intrinsic term dominates when $\omega_1 + \omega_2 \gg \omega_1$ or ω_2 . The intrinsic term, which is exact for the infinite plane and noninteracting electrons is the central result of this Letter. To address experimental feasibility we must consider the role of contacts as well as electron-electron interactions. These both introduce complications into the analysis.

As a model for electrical contacts, consider Fig. 3, which depicts a 2DEG of size L with large area tunnel contacts to ideal metallic leads separated by a distance b . Provided the capacitance between the contacts and the 2DEG is sufficiently large, the voltages in the leads will establish a potential profile in the 2DEG as in Eq. (11). We assume the tunnel barrier is in a regime in which the mean free path ℓ for tunneling from the 2DEG to the leads satisfies $k_F^{-1} \ll \ell \ll L$. This defines a dwell time $\tau = \ell/v_F$ for electrons in the 2DEG. In the pulse construction, we clearly require $t_{21} < \tau$, since for $t_{21} > \tau$ the first pulse has disappeared before the second arrives. In the frequency domain calculation, tunneling to the leads introduces an exponential decay $e^{-|r|/\ell}$ into $D(\mathbf{r}, \mathbf{k}, \omega)$, which cuts off the small ω_1 divergence in α , effectively replacing $\omega_1 \rightarrow \omega_1 + i/\tau$. The coupling to the leads therefore places a lower bound $\omega_1, \omega_2 \gg \omega_c$ for the applicability of (2) with $\omega_c \sim \tau^{-1}$. The intrinsic behavior is thus recovered when $\omega_c \ll \omega_{1(2)} \ll \omega_{2(1)}$.

A second complication involves the role of electron-electron interactions. In 1D, the analog of our calculation is the Kubo formula conductance G_{Kubo} , which is given by $G_{\text{Kubo}} = Ke^2/h$, where $K < 1$ is the Luttinger parameter characterizing repulsive electron interactions [25,26]. However, G_{Kubo} does not correctly account for the electrical contacts, and it was argued that for Fermi liquid leads on a

1DEG of length L , $G(\omega) = e^2/h$ for $\omega \ll v_F/L$ [27–32]. An appealing interpretation of this was explained by Kawabata [33], who argued that G_{Kubo} computed in an infinite system is renormalized because it describes the response to the *applied* voltage, while the quantized conductance, which reflects the chiral anomaly, is the response to the *self-consistent* potential, which includes screening due to interactions. Moreover, for the dc conductance, it is the self-consistent potential that determines the measured electrochemical potential difference. Shimizu [34] emphasized the similarity of this description to Fermi liquid theory [35]. In terms of Feynman diagrams, for the response to the applied field, the Kubo formula bubble diagram [Fig. 2(c)] is dressed by convolving with RPA-like polarization bubbles [Fig. 2(d)], $\Pi(x, \omega)$, represented here in real space. For a 1DEG in which leads are modeled by setting the interactions to zero for $|x| > L$, it can be checked that, since $\Pi(x, \omega) \sim (\omega/v_F)e^{i\omega x/v_F}$ and $|x| < L$, the interaction corrections vanish for $\omega \ll v_F/L$.

To incorporate electron interactions into the calculation of the 2D nonlinear response, we adopt a renormalized Fermi liquid description [36] in which quasiparticles near E_F interact with an energy $f_{\mathbf{k}\mathbf{k}'}n_{\mathbf{k}}n_{\mathbf{k}'}$, where $n_{\mathbf{k}} = c_{\mathbf{k}}^\dagger c_{\mathbf{k}}$. At low energy, the important interaction corrections involve RPA bubbles [37], and summing the diagrams like in Fig. 2(e) is equivalent to incorporating the Fermi liquid interactions $f_{\mathbf{k}\mathbf{k}'}$ into the Boltzmann equation [35,36]. This is difficult to solve, in general, but by evaluating the simplest diagram at first order in $f_{\mathbf{k}\mathbf{k}'}$ it can be checked that the response to the applied field is modified: $\chi_F \rightarrow \chi_F + O[N(E_F)f]$, where f is an average of $f_{\mathbf{k}\mathbf{k}'}$ over the Fermi surface. Thus, the nonlinear response in 2D is modified by the Fermi liquid parameters just as the linear response in 1D is modified by the Luttinger parameter. The bubble $\Pi(\omega, \mathbf{r}) \propto (\omega/v_F)e^{i\omega|\mathbf{r}|/v_F}$ vanishes for $\omega \ll \omega_c$ as for $D = 1$. However, since we must consider $\omega_1, \omega_2 \gg \omega_c$, the interaction corrections remain. The origin of the correction is the same as in $D = 1$: due to interactions, the potential is screened, as is accounted for by the RPA bubbles.

At finite frequency, more detailed modeling is required to determine the relation between the self-consistent potential and the measured voltage. In the absence of that, it will be fruitful to consider weakly interacting systems. Consider a 2D Dirac material, such as graphene, with density of states $N(E) \sim |E|/v_F^2$. For a short-ranged interaction (screened by the leads) $N(E_F)f \ll 1$ for sufficiently small E_F . Interestingly, the Fermi surface is electron-like (hole-like) for $E_F > 0$ ($E_F < 0$), so the response characterized by $\chi_F = 4\text{sgn}E_F$ (including spin and valley) changes sign at charge neutrality.

Our analysis opens several avenues for further inquiry. On the practical side, it will be interesting to search for other measurable quantities that probe χ_F . Promising candidates include low frequency current noise as well

as thermal conductance. It will also be interesting to generalize our theory to $D > 2$ and to explore ways in which χ_F provides a fundamental characterization of a degenerate Fermi gas. Our analysis suggests that χ_F defines a kind of “higher order” anomaly. In 1D, the chiral anomaly characterizes the connection between left- and right-moving electrons, which leads to a lack of conservation of the right movers. For $D > 1$, χ_F characterizes a more general violation of conservation due to the fact that electrons propagating in different directions are connected at critical points \mathbf{k}_m . This is related to the Fermi surface anomaly discussed in Ref. [38], which characterizes a particular point on the Fermi surface. However, unlike that description, χ_F provides a global characterization of the Fermi surface. For $D = 1$ the bipartite entanglement entropy has a universal term $S = (c/3) \log L$ [39,40] with $c = \chi_F$. This has been generalized to higher D , where S describes a logarithmic area law entanglement that involves the projected area of the Fermi surface [41,42], which is nonzero even for a system of decoupled 1D wires [43], with $\chi_F = 0$. We speculate that, for $D > 1$, χ_F shows up in an intrinsically D -dimensional entanglement measure.

We thank Patrick Lee and Pok Man Tam for helpful suggestions. This work was supported by a Simons Investigator Grant from the Simons Foundation.

-
- [1] K. v. Klitzing, G. Dorda, and M. Pepper, New Method for High-Accuracy Determination of the Fine-Structure Constant Based on Quantized Hall Resistance, *Phys. Rev. Lett.* **45**, 494 (1980).
- [2] D. J. Thouless, M. Kohmoto, M. P. Nightingale, and M. den Nijs, Quantized Hall Conductance in a Two-Dimensional Periodic Potential, *Phys. Rev. Lett.* **49**, 405 (1982).
- [3] F. D. M. Haldane, Berry Curvature on the Fermi Surface: Anomalous Hall Effect as a Topological Fermi-Liquid Property, *Phys. Rev. Lett.* **93**, 206602 (2004).
- [4] F. de Juan, A. Grushin, T. Morimoto, and J. E. Moore, Quantized circular photogalvanic effect in Weyl semimetals, *Nat. Commun.* **8**, 15995 (2017).
- [5] A. Avdoshkin, V. Kozii, and J. E. Moore, Interactions Remove the Quantization of the Chiral Photocurrent at Weyl Points, *Phys. Rev. Lett.* **124**, 196603 (2020).
- [6] N. W. Ashcroft and N. D. Mermin, *Solid State Physics* (Saunders College, Fort Worth, 1976).
- [7] I. M. Lifshitz, Anomalies of electron characteristics of a metal in the high pressure region, *Sov. Phys. JETP* **11**, 1130 (1960).
- [8] G. E. Volovik, Topological Lifshitz transitions, *Low Temp. Phys.* **43**, 47 (2017).
- [9] G. E. Volovik, Exotic Lifshitz transitions in topological materials, *Phys. Usp.* **61**, 89 (2018).
- [10] R. Landauer, Spatial variation of currents and fields due to localized scatterers in metallic conduction, *IBM J. Res. Dev.* **1**, 223 (1957).
- [11] D. S. Fisher and P. A. Lee, Relation between conductivity and transmission matrix, *Phys. Rev. B* **23**, 6851 (1981).
- [12] B. J. van Wees, H. van Houten, C. W. J. Beenakker, J. G. Williamson, L. P. Kouwenhoven, D. van der Marel, and C. T. Foxon, Quantized conductance of point contacts in a two-dimensional electron gas, *Phys. Rev. Lett.* **60**, 848 (1988).
- [13] T. Honda, S. Tarucha, T. Saku, and Y. Tokura, Quantized conductance observed in quantum wires 2 to 10 μm long, *Jpn. J. Appl. Phys.* **34**, L72 (1995).
- [14] I. van Weperen, S. R. Plissard, E. P. A. M. Bakkers, S. M. Frolov, and L. P. Kouwenhoven, Quantized conductance in an InSb nanowire, *Nano Lett.* **13**, 387 (2013).
- [15] S. Frank, P. Poncharal, Z. L. Wang, and W. A. de Heer, Carbon nanotube quantum resistors, *Science* **280**, 1744 (1998).
- [16] M. Nakahara, *Geometry, Topology and Physics*, Graduate Student Series in Physics (Hilger, Bristol, 1990).
- [17] J. Milnor, *Morse Theory (AM-51)*, Volume 51 (Princeton University Press, Princeton, NJ, 1969).
- [18] C. Nash and S. Sen, *Topology and Geometry for Physicists* (Academic Press, New York, 1988).
- [19] R. B. Laughlin, Quantized Hall conductivity in two dimensions, *Phys. Rev. B* **23**, 5632 (1981).
- [20] W. Kraut and R. von Baltz, Anomalous bulk photovoltaic effect in ferroelectrics: A quadratic response theory, *Phys. Rev. B* **19**, 1548 (1979).
- [21] R. von Baltz and W. Kraut, Theory of the bulk photovoltaic effect in pure crystals, *Phys. Rev. B* **23**, 5590 (1981).
- [22] Y. Zhang, H. Ishizuka, J. van den Brink, C. Felser, B. Yan, and N. Nagaosa, Photogalvanic effect in Weyl semimetals from first principles, *Phys. Rev. B* **97**, 241118(R) (2018).
- [23] See Supplemental Material at <http://link.aps.org/supplemental/10.1103/PhysRevLett.128.076801> for a derivation of Eq. (15), as well as the evaluation of (15) for a triple point contact.
- [24] If one of the angles φ_p is greater than π , α_i is still quantized, but its value is modified. See Supplemental Material Sec. B [23], where it is also established that for Fig. 1(a) the pulse argument analysis remains valid.
- [25] W. Apel and T. M. Rice, Combined effect of disorder and interaction on the conductance of a one-dimensional fermion system, *Phys. Rev. B* **26**, 7063 (1982).
- [26] C. L. Kane and M. P. A. Fisher, Transport in a One-Channel Luttinger Liquid, *Phys. Rev. Lett.* **68**, 1220 (1992).
- [27] D. L. Maslov and M. Stone, Landauer conductance of Luttinger liquids with leads, *Phys. Rev. B* **52**, R5539 (1995).
- [28] V. V. Ponomarenko, Renormalization of the one-dimensional conductance in the Luttinger-liquid model, *Phys. Rev. B* **52**, R8666 (1995).
- [29] I. Safi and H. J. Schulz, Transport in an inhomogeneous interacting one-dimensional system, *Phys. Rev. B* **52**, R17040 (1995).
- [30] I. Safi, Conductance of a quantum wire: Landauer’s approach versus the Kubo formula, *Phys. Rev. B* **55**, R7331 (1997).
- [31] I. Safi, A dynamic scattering approach for a gated interacting wire, *Eur. Phys. J. B* **12**, 451 (1999).
- [32] R. Thomale and A. Seidel, Minimal model of quantized conductance in interacting ballistic quantum wires, *Phys. Rev. B* **83**, 115330 (2011).
- [33] A. Kawabata, On the renormalization of conductance in Tomonaga-Luttinger liquid, *J. Phys. Soc. Jpn.* **65**, 30 (1996).

- [34] A. Shimizu, Landauer conductance and nonequilibrium noise of one-dimensional interacting electron systems, *J. Phys. Soc. Jpn.* **65**, 1162 (1996).
- [35] D. Pines and P. Nozieres, *The Theory of Quantum Liquids* (CRC Press, Boca Raton, FL, 1966).
- [36] R. Shankar, Renormalization-group approach to interacting fermions, *Rev. Mod. Phys.* **66**, 129 (1994).
- [37] H. Rostami, M. I. Katsnelson, and M. Polini, Theory of plasmonic effects in nonlinear optics: The case of graphene, *Phys. Rev. B* **95**, 035416 (2017).
- [38] D. V. Else, R. Thorngren, and T. Senthil, Non-Fermi Liquids as Ersatz Fermi Liquids: General Constraints on Compressible Metals, *Phys. Rev. X* **11**, 021005 (2021).
- [39] C. Holzhey, F. Larsen, and F. Wilczek, Geometric and renormalized entropy in conformal field theory, *Nucl. Phys.* **B424**, 443 (1994).
- [40] P. Calabrese and J. Cardy, Entanglement entropy and quantum field theory, *J. Stat. Mech.* **2004**, P06002 (2004).
- [41] D. Gioev and I. Klich, Entanglement Entropy of Fermions in Any Dimension and the Widom Conjecture, *Phys. Rev. Lett.* **96**, 100503 (2006).
- [42] B. Swingle, Entanglement Entropy and the Fermi Surface, *Phys. Rev. Lett.* **105**, 050502 (2010).
- [43] W. Ding, A. Seidel, and K. Yang, Entanglement Entropy of Fermi Liquids via Multidimensional Bosonization, *Phys. Rev. X* **2**, 011012 (2012).